HHS Public Access

Author manuscript

Oncogene. Author manuscript; available in PMC 2013 May 08.

Published in final edited form as:

Oncogene. 2012 November 8; 31(45): 4740–4749. doi:10.1038/onc.2011.636.

RhoA triggers a specific signaling pathway that generates transforming microvesicles in cancer cells

Bo Li, BS[1,2,3], **Marc A. Antonyak, PhD**[1,3], **Jingwen Zhang, BS**[1], and **Richard A. Cerione, PhD**[1,2]

[1]Department of Molecular Medicine, Cornell University, Ithaca, NY 14853, USA

[2]Department of Chemistry and Chemical Biology, Baker Laboratory, Cornell University, Ithaca, NY 14853, USA

Abstract

Vesicular structures called microvesicles (MV) that are shed from the surfaces of cancer cells are capable of transferring oncogenic cargo to recipient cancer cells, as well as to normal cells, sending mitogenic signals that greatly enhance tumor growth. Because MVs are stable in the circulation, they also may play a key role in secondary colonization and metastasis. Thus, understanding how MVs are generated could have important consequences for interfering with cancer progression. Here we report that the small GTPase RhoA triggers a specific signaling pathway essential for MV biogenesis in various human cancer cells. Inhibiting the activity of different proteins comprising this pathway blocks MV biogenesis in the donor cancer cells and prevents oncogenic transformation in cell culture as well as tumor growth in mice. While RhoA has often been implicated in human cancer, these findings now highlight a previously unappreciated role for this GTPase in malignant transformation, and demonstrate that blocking MV biogenesis may offer novel approaches for interfering with malignant transformation.

Keywords

microvesicles; oncosomes; RhoA; ROCK; LIMK; tissue transglutaminase

Introduction

Classical cell-cell communication involves the secretion of growth factors, hormones, or cytokines that stimulate signaling activities within cells in either an autocrine or paracrine fashion upon binding to their cell-surface receptors. Although these secretory events have been commonly assumed to serve as the predominant mode of cell-cell communication, a novel type of vesicle secretion, referred to as microvesicles (MVs) or oncosomes (when shed from cancer cells), has begun to receive a great deal of attention[1-4]. Microvesicles

Correspondence: Richard A. Cerione, Department of Molecular Medicine, College of Veterinary Medicine, Cornell University, Ithaca, NY 14853-6401. Tel: (607) 253-3888, Fax: (607) 253-3659, rac1@cornell.edu.

[3]These authors contributed equally to this work

Conflict of Interest The authors declare no conflict of interest.

(MVs) are unconventional cellular secretory structures that contain an array of cargo including cell surface receptors and other signaling proteins, extracellular matrix remodeling proteins, as well as mRNA transcripts and microRNAs[1-6]. They have sometimes been mistakenly identified as exosomes, which are conventional secretory vesicles generated through the classical endosome - multivesicular body (MVB) trafficking pathway[7]. However, MVs are distinct from exosomes with regard to how they are generated, as well as their size, lipid composition, and cargo[8].

There has been a growing appreciation that MVs play important roles in cancer progression, as several malignant cancer cell lines exhibit enhanced production of MVs that influence the tumor microenvironment as well as stimulate angiogenesis and promote tumor growth[2,3,5,6,9]. Moreover, MVs shed from cancer cells have been shown to help generate a more “tumor-friendly” niche through the actions of some of their cargo such as metallo-proteases, or by directly stimulating signaling activities within recipient cells following the transfer of their cargo[10,11]. For example, the expression of a mutated form of the EGF receptor, EGFRvIII, in glioblastomas stimulated the formation of MVs that upon engaging neighboring glioblastoma cells, gave rise to enhanced EGFR-signaling and oncogenic transformation within the recipient cancer cells[1]. Remarkably, MVs derived from cancer cells are also capable of conferring onto normal cells, the characteristics of transformed cells[3]. Thus, given the potentially important roles played by MVs in malignant transformation, it is of great interest to understand the nature of the signaling pathway responsible for their biogenesis.

In the present study, we set out to delineate the signals responsible for MV biogenesis in two different types of cancer cells, MDAMB231 breast cancer cells and HeLa cervical carcinoma cells. We show that the formation of MVs is an outcome of a specific Rho GTPase-dependent signaling pathway that is activated in HeLa cells by EGF and is constitutively activated in MDAMB231 cells. This pathway triggers the activation of Rho kinase (ROCK), and subsequently Lim kinase (LIMK), culminating in the phosphorylation of cofilin. We further demonstrate that the hyper-activation of this signaling pathway and the resultant generation of MVs have a significant impact on tumor formation in mice. In light of the roles suggested for Rho GTPases and ROCK in cancer cell migration, invasion, and the development of the metastatic state[12], these findings carry exciting implications regarding how these signaling proteins might contribute to malignant transformation.

Results

Human cancer cells generate MVs that are capable of inducing transformation

MVs can be seen decorating the surfaces of highly aggressive MDAMB231 breast cancer cells, as visualized by scanning electron microscopy (Figure 1a), as well as by immunofluorescence when staining for tissue transglutaminase (tTG) (Figure 1b), a protein crosslinking enzyme that is over-expressed in human cancers and is a major MV protein component[3,13,14]. They can also be visualized by rhodamine phalloidin staining of filamentous actin (F-actin) (Figure 1b). Similarly, MVs were observed on highly aggressive U87 glioblastoma cells even in the absence of any extracellular stimuli, whereas, their

formation was induced by EGF in human cervical carcinoma (HeLa) cells (Figure 1b). They were found on ~25-40% of MDAMB231, U87, and EGF-stimulated HeLa cells (Figure 1c).

Microvesicles can be isolated from the conditioned medium of cancer cells, as detected by Western blotting using tTG and actin antibodies, as well as with an antibody that recognizes flotillin-2, a general MV-marker protein (Figure 1d)[1,3]. The cytosolic protein IκBα was absent from these MV preparations, verifying the lack of cytosolic contamination. In HeLa cells, MVs could only be collected from cells treated with EGF (Figure 1e), consistent with our immunofluorescence studies (Figures 1b and 1c). The ectopic expression of a dominant-negative mutant of the CHMP3 protein (CHMP3 DN), the mammalian homolog of the yeast VPS24 protein that is essential for the secretion of exosomes[15], did not reduce the amount of MVs collected from MDAMB231 cells (Figure S1a), indicating that MVs and exosomes are distinct species.

We recently reported that incubating normal (non-transformed) NIH3T3 fibroblasts with MVs isolated from cancer cells induced the transformation of the recipient fibroblasts[3]. Here we show examples of the transforming capability of MVs collected from MDAMB231 and U87 cells, as well as from EGF-treated HeLa cells (Figures S1b and S1c).

We have also examined the ability of cancer cell-derived MVs to induce tumor formation, using the protocol outlined in Figure 2a. Specifically, MDAMB231 cells are first treated with the mitosis-arresting agent mitomycin C, which blocks their ability to induce tumors while still allowing these cells to generate and shed MVs. The treated cancer cells are then injected alone, or together with NIH3T3 cells, into nude mice. Figure 2b presents the results of such an experiment. Neither the mitomycin C-treated cancer cells nor NIH3T3 cells, alone, induced tumors, whereas fibroblasts exposed to MVs shed from the treated cancer cells formed tumors in 3 out of 6 animals. We then went on to determine whether these tumors were primarily comprised of NIH3T3 mouse fibroblasts (rather than MDAMB231 human breast cancer cells), as would be expected if the MVs induced the aberrant growth of the fibroblasts, by taking advantage of an antibody that recognizes the mouse, but not human, form of the Cool-1/β-Pix protein (Figure 2c, compare lanes 1 and 2). Subjecting lysates of the tumors to Western blot analysis using this antibody, we found that Cool-1/β-Pix could be detected in each of the tumors (Figure 2c, see the last 3 lanes), suggesting that the resulting tumor masses were due to the MV-stimulated growth of the NIH3T3 cells.

Given the indications that cancer cell-derived MVs play critical roles in malignant transformation, a key question then becomes the underlying mechanistic basis for their biogenesis. Because MV production in HeLa cells is triggered by EGF, we used these cells as a model system to identify the signaling proteins acting downstream of the EGFR in this process. The fact that MVs are characterized by “actin-ring” structures (Figure 1b), prompted us to consider the potential roles of Ras, Rac, Rho, and Cdc42, as these GTPases are known for their abilities to reorganize the actin cytoskeleton upon EGF stimulation[16,17]. The vector-alone or HA-tagged, dominant-active forms of Rac (Rac F28L), Cdc42 (Cdc42 F28L), Ras (Ras G12V), or RhoA (RhoA F30L) were expressed in HeLa cells, and then MVs were visualized along the surfaces of the transfectants by immunostaining with tTG and HA antibodies. It is worth noting that each of these constructs expressed similarly in the

cells, as determined by Western blot analysis (Figure S2), suggesting that the inability of any of these small GTPases to generate MVs is likely not an outcome of their insufficient expression. Figures 3a (left-hand column) and 3b show that neither activated Rac, Cdc42, nor Ras, was able to induce MV formation in HeLa cells, as detected by immunofluorescence using a tTG antibody. However, cells expressing the constitutively-active RhoA (F30L) mutant exhibited significant MV formation. Likewise, cells expressing RhoA (F30L) yielded increased amounts of MVs in the conditioned medium (Figure 3c). Knocking-down RhoA by siRNA abolished the EGF-stimulated shedding of MVs from HeLa cells (Figure 3d). Similar results were obtained in MDAMB231 cells (Figure 3e).

The ability of MDAMB231 cells to constitutively produce MVs, while HeLa cells required EGF stimulation to generate them, was well correlated with the activation status of RhoA in these cells. Specifically, RhoA was constitutively activated in MDAMB231 cells, whereas its activation in HeLa cells was dependent upon EGF treatment (Figure 3f). Interestingly, RhoC was ineffective in generating MVs despite the fact that it expresses reasonably well in HeLa cells (Figure S2, last lane) and shares a high degree of sequence similarity with RhoA (Figure 3g). The over-expression of dominant-active Arf6 (Arf6 Q67L) was also unable to mimic the actions of RhoA in HeLa cells, suggesting that the reported effects of Arf6 on the shedding of MVs from cells[18] do not directly involve their actual biogenesis. MV formation is also not a general outcome of oncogenic signaling, as it was not triggered in HeLa cells expressing an activated form of the Src tyrosine kinase (Src Y527F) (Figure 3g).

ROCK is downstream from RhoA in the pathway leading to MV formation

Several signaling targets have been identified for activated RhoA, with the protein kinases ROCK-1 and ROCK-2 (for Rho-associated coiled coil-containing kinases 1 and 2) having been implicated in actin cytoskeletal remodeling and actomyosin contraction[12]. Thus, we examined their roles in MV formation by taking advantage of the small molecule Y-27632, which inhibits both ROCK-1 and ROCK-2 kinase activity[19]. Figures 4a and 4b show that treatment of MDAMB231, U87, or EGF-stimulated HeLa cells with Y-27632 eliminated the appearance of MVs along their surfaces. Similarly, the amount of MVs collected from the conditioned medium of MDAMB231 or U87 cells was markedly reduced upon Y-27632 treatment (Figure 4c).

To determine whether ROCK-1 or ROCK-2 specifically mediates the actions of RhoA in MV formation, we knocked down the expression of each ROCK isoform using specific ROCK-1 or ROCK-2 siRNAs. Under conditions where we achieved an ~50% knock-down of the two ROCK isoforms (Figures S3a and S3b), we saw only minor reductions in the amount of MVs collected from these cancer cells (Figures S3c and S3d). This suggested that both ROCK-1 and ROCK-2 might be capable of triggering MV formation, consistent with these two isoforms sharing a number of common targets[20]. However, while attempts to achieve the simultaneous knock-down of both ROCK isoforms have been unsuccessful, we found that ectopically expressing a kinase-defective, dominant-negative mutant of either ROCK-1 (ROCK-1 DN) or ROCK-2 (ROCK-2 DN) in MDAMB231 cells led to marked decreases in MV formation (Figure S3e). These data suggested that ROCK-1 and -2 function in a redundant manner in promoting MV formation in cancer cells. We then examined

whether the over-expression of ROCK was sufficient to drive MV formation in cancer cells. Thus far, we have only obtained significant ectopic expression of Myc-tagged ROCK-2 in HeLa cells (Figure 4d, WCL), but this was sufficient to trigger MV formation in HeLa cells, similar to what we see when ectopically expressing the constitutively active RhoA F30L mutant (Figures 4e and 4f). Likewise, the over-expression of ROCK-2 increased the amount of MVs isolated from the culturing medium of HeLa cells (Figure 4d, MV).

MV formation in cancer cells is dependent on a Lim kinase-cofilin signaling pathway activated by ROCK

LIM-kinase (LIMK) and Myosin light chain phosphatase (MYLP) are two well-studied signaling targets immediately downstream from ROCK that regulate actin cytoskeletal dynamics (Figure 5a)[21-23]. Activated ROCK phosphorylates LIMK, stimulating its kinase activity and enabling it to phosphorylate Ser3 on cofilin, which prevents cofilin from severing actin filaments and prolongs the extension of actin fibers[23]. ROCK also inhibits MYLP activity through the direct phosphorylation of the myosin phosphatase-targeting subunit (MYPT), resulting in an enhancement of myosin phosphorylation and actomyosin contraction[21]. Figure 5b shows that the treatment of HeLa cells with EGF significantly increased the phosphorylation of LIMK and myosin, with each of these phosphorylation events being antagonized by the ROCK inhibitor Y-27632. We then examined whether the over-expression of LIMK in HeLa cells, or the increased phosphorylation of myosin that occurs when over-expressing myosin light chain kinase (MYLK), mimicked the ability of ROCK to stimulate MV formation. Interestingly, we found that while the over-expression of MYLK caused only a modest increase in MV formation (data not shown), the ectopic expression of wild-type LIMK (LIMK WT) in HeLa cells generated MVs to an extent comparable to RhoA F30L (Figures 5c and 5d). The over-expression of LIMK also gave rise to MVs that were shed into the conditioned medium of HeLa cells similar to cells expressing RhoA F30L (Figure 5e).

We then examined whether the LIMK D460N mutant, that is defective for protein kinase activity[23], might act as a dominant-negative inhibitor of MV formation. Figure 5f shows that the co-expression of LIMK D460N together with RhoA F30L in HeLa cells significantly suppressed the ability of RhoA to induce MV formation, whereas co-expressing RhoA F30L with the MYLK ATPDEL mutant, which is kinase-defective because of an internal deletion that prevents the binding of ATP[24], had little, if any inhibitory effect (Figure 5f).

We next investigated the role of cofilin, the major downstream effector of LIMK, in MV formation. We generated a dominant-active form of cofilin (cofilin S3A), which was incapable of being phosphorylated by LIMK[23], and found that its over-expression in HeLa cells severely impaired the ability of EGF to stimulate MV formation (Figure 5g, the arrows in the top-left panel point to MVs forming on a cell that does not express cofilin S3A; also, see Figure 5h). The same was true when ectopically expressing the cofilin S3A mutant in MDAMB231 cells, as it strongly reduced the amount of MVs isolated from these cancer cells, similar to the phosphorylation-defective LIMK D460N mutant (Figure 5g, bottom row, and Figure 5i).

RhoA signaling to LIMK and cofilin is essential for MV-mediated transformation

To further confirm the significance of LIMK, we collected MVs from MDAMB231 cells that stably expressed a control siRNA, or two LIMK-targeted siRNAs. As expected, the effectiveness of the LIMK knock-downs (Figure 6a) were inversely correlated with the amount of MVs isolated from MDAMB231 cells (Figure 6b) and, in a corresponding manner, with the extent of anchorage-independent growth that these vesicle preparations were able to induce in NIH3T3 cells (Figure 6c). We then set out to establish the importance of LIMK for tumor formation in mice, using a similar strategy as that utilized to initially establish a role for MVs in this process (Figure 2a; also, ref. 3). Specifically, MDAMB231 cells expressing a control siRNA or the siRNAs targeting LIMK were mitotically-arrested with mitomycin C, and then the treated breast cancer cells were injected together with NIH3T3 cells into nude mice. Figures 6d and 6e show that the stable knock-down of LIMK expression in mitotically-arrested MDAMB231 cells markedly suppressed the ability of co-injected NIH3T3 fibroblasts to form tumors.

Discussion

Tumorigenesis requires the communication of cancer cells with the tumor microenvironment[25], as mediated by MVs to promote extracellular matrix remodeling, as well as to stimulate blood vessel formation, recruit tumor-associated macrophages, activate surrounding tumor cells, and induce transformed phenotypes within neighboring normal cells[2,3,6,7]. Here we highlight a RhoA/ROCK-dependent signaling pathway that culminates in the formation of MVs in cancer cells and thus holds significant consequences for tumorigenesis (Figure 6f). We further show that LIMK activity, through its ability to phosphorylate cofilin and inhibit its actin-severing activity, is both necessary and sufficient for the biogenesis of MVs in cancer cells. Presumably, the resultant elongation of actin filaments along the plasma membranes leads to the formation of an “actin-ring” structure that serves as an essential step for the maturation of MVs. A potential role for LIMK as an oncogene has been suggested previously, based on its ability to phosphorylate cofilin and to stimulate cell proliferation and tumor growth[26-28]. Moreover, LIMK has been linked to the development of metastasis[27,29]. Likewise, RhoA and ROCK have been frequently implicated in cancer metastasis through their regulation of cell migration and their ability to stimulate an amoeboid mode of invasion[30-32]. The critical roles played by RhoA, ROCK, and LIMK in MV formation now shed new light on how these signaling proteins contribute to the progression of a number of different human cancers.

One of the most striking aspects of MV biogenesis in cancer cells is the signaling specificity that underlies this process. While activated RhoA is extremely effective at triggering MV formation, none of the other members of the Rho GTPase family thus far examined, including RhoC, which is highly similar to RhoA and has also been implicated in cancer progression and metastasis[30], is effective in stimulating MV formation. This implies that the RhoA-signaling pathway responsible for these events is assembled with a high degree of temporal and spatial precision. One intriguing possibility is that this signaling pathway is linked to the formation of another type of membrane structure, referred to as plasma membrane blebs (PM blebs)[33,34]. PM blebs are initiated by the disruption of membrane-

actomyosin interactions, which results in a rapid protrusion of the plasma membrane[35]. The subsequent steps in bleb formation involve the recruitment of the actomyosin machinery beneath the detached membrane, the *in situ* build-up of new actin cortex, as well as the final retraction of the mature blebs[35]. PM blebs share some intriguing similarities with MVs, including an identical "actin-ring" phenotype, raising the possibility that PM blebs and MVs arise through a common mechanism, with the distinction being that those membrane structures undergoing inward contraction represent PM blebs, whereas those that are shed outward from the cell surface are secreted MVs. If indeed MVs represent the opposite outcome of PM blebs, then it will be of great interest to learn more about how these distinct events are mediated, and whether the regulation of MV versus bleb formation is altered in cancer cells relative to their normal cellular counterparts, as re-setting their regulatory mechanisms in transformed cells could offer important strategies for interfering with tumor progression.

Materials and Methods

Materials

All cell culture reagents, EGF, Oregon green- and Texas red-conjugated secondary IgGs, rhodamine-conjugated phalloidin, Lipofectamine, Lipofectamine 2000, as well as the control, and gene-specific siRNAs were from Invitrogen. Y-27632 and 4,6-diamidino-2-phenylindole (DAPI) were from Calbiochem. The tTG and actin antibodies were from Lab Vision/Thermo, the flotillin-2 and ROCK-1 and -2 antibodies were from Santa Cruz, the Cool-1/β-Pix antibody was from BD Biosciences, while the HA and Myc antibodies were from Covance. The antibodies against IκBα, RhoA, LIMK, phospho-LIMK, MLC, and phospho-MLC were all from Cell Signaling. The RhoA activation assay Biochem Kit was from Cytoskeleton, while the 0.22 μm pore size Steriflip PVDF filters were from Millipore.

Expression plasmids

Human RhoA, RhoC, Rac, Ras, Cdc42, Src, ROCK-1, ROCK-2, LIMK, MYLK, Cofilin, and CHMP3 were cloned into a Myc- or HA-tagged PCDNA3 expression vector. Site-directed mutagenesis was used to generate the various mutants used in this study.

Cell Culture

HeLa, MDAMB231 and U87 cell lines were grown in RPMI 1640 medium containing 10% fetal bovine serum, and NIH3T3 cells were maintained in DMEM medium containing 10% calf serum (CS). The expression constructs were transfected into cells using Lipofectamine, while the siRNAs were introduced into cells using Lipofectamine 2000. Where indicated, cells were treated with 0.1 μg/ml EGF or 5 μM Y-27632. To mitotically arrest cells, plates of cells were treated with 10 μg/ml mitomycin C for 2 hours, before being rinsed away and allowed to recover in the growth medium for a day.

Isolation of MVs from Cancer Cells

MVs were isolated from the conditioned medium of cancer cells as previously described[3]. Briefly, the medium collected from two nearly confluent 150 mm dishes of serum-starved cells was subjected to two centrifugations; the first at 300 g for 10 minutes pelleted floating

cells, while the second at 12,000 g for 20 minutes pelleted cell debris. The supernatant was then subjected to a third centrifugation at 100,000 g for 1.5 hours, and the resulting pellet was lysed in cell lysis buffer (25 mM Tris, 100 mM NaCl, 1% Triton X-100, 1 mM EDTA, 1 mM DTT, 1 mM $NaVO_4$, 1 mM β-glycerol phosphate, and 1 μ1g/mL aprotinin). To prepare the intact MVs to be used in the anchorage-independent growth assays (see below), the conditioned medium collected from serum-starved or EGF-stimulated cancer cells was cleared of intact cells and cell debris, and then filtered through a Millipore Steriflip PVDF-filter. The MVs retained by the filter were then resuspended in serum-free medium.

Immunoblot Analysis

Cells, MVs, and tumors were lysed with cell lysis buffer, and the lysates were resolved by SDS-PAGE and transferred to PDVF membranes. The membranes were incubated with various primary antibodies diluted in TBST (20 mM Tris, 135 mM NaCl, and 0.05% Tween 20), and then with horseradish peroxidase-conjugated secondary antibodies followed by exposure to ECL reagent.

Immunofluorescence

Cells ectopically expressing the various constructs, or treated with different reagents as indicated, were fixed with 3.7% formaldehyde, permeabilized with 0.2% Triton X-100, and then blocked with 10% bovine serum albumin. The cells were then incubated with primary antibodies, followed by incubation with a fluorophore-conjugated secondary antibody. Rhodamine-conjugated phalloidin was used to label actin filaments and DAPI was used to stain nuclei. The samples were visualized using a fluorescent microscope and the images were captured using IPlab software.

Scanning Electron Microscopy (SEM)

MDAMB231 cells grown on Lab-Tek chamber slides (Nunc/Lab Vision) were fixed for 1 hour with 2% EM-grade glutaraldehyde diluted in 0.05 M cacodylic acid buffer solution (PH=7.4), and then for an additional hour with PBS containing 1% osmium tetroxide. The samples were first dehydrated in gradient solutions of 25%, 50%, 70%, 95%, and 100% ethanol, and then using the CPD-30 critical point drying machine (BAL-TEC SCD050). The samples were then sputter-coated with a thin-layer of platinum, before being observed using a Leica 440 Scanning Electron Microscope.

Anchorage-independent Growth Assays

NIH3T3 cells incubated without or with MVs derived from 5.0×10^6 serum-starved or EGF-stimulated MDAMB231, U87, or HeLa cells were plated at a density of 7,000 cells/mL in DMEM medium containing 0.3% agarose and 10% CS, onto underlays composed of 10% CS and 0.6% agarose in 6-well dishes. The soft agar cultures were re-fed with freshly prepared MVs and CS every fourth day for 12 days, at which time the colonies that formed were counted. Each of the assays was performed 3 times and the results were averaged together and graphed.

Mouse Studies

1×10^6 mitotically arrested (using mitomycin C) parental MDAMB231 cells or MDAMB231 cells stably expressing control or LIMK siRNAs were combined with 1×10^6 NIH3T3 fibroblasts and Matrigel (BD Biosciences) to achieve 30% Matrigel in the final solution. The cell preparations were subcutaneously injected into the flanks of 6-8 weeks-old female NIH-III nude mice. As controls, naive MDAMB231, MDAMB231 cells expressing the control siRNA cells, and NIH3T3 cells were combined with Matrigel and injected into mice as well. Two months later, the animals were sacrificed and the resulting tumors were excised and weighed.

Supplementary Material

Refer to Web version on PubMed Central for supplementary material.

Acknowledgments

We thank Cindy Westmiller for her secretarial assistance and the NIH and the Komen Foundation for funding.

REFERENCES

1. Al-Nedawi K, Meehan B, Micallef J, Lhotak V, May L, Guha A, et al. Intercellular transfer of the oncogenic receptor EGFRvIII by microvesicles derived from tumour cells. Nat Cell Biol. 2008; 10:619–624. [PubMed: 18425114]
2. Al-Nedawi K, Meehan B, Rak J. Microvesicles: messengers and mediators of tumor progression. Cell Cycle. 2009; 8:2014–2018. [PubMed: 19535896]
3. Antonyak MA, Li B, Boroughs LK, Johnson JL, Druso JE, Bryant KL, et al. Cancer cell-derived microvesicles induce transformation by transferring tissue transglutaminase and fibronectin to recipient cells. Proc Natl Acad Sci USA. 2011; 108:4852–4857. [PubMed: 21368175]
4. Skog J, Wurdinger T, van Rijn S, Meijer DH, Gainche L, Sena-Esteves M, et al. Glioblastoma microvesicles transport RNA and proteins that promote tumour growth and provide diagnostic biomarkers. Nat Cell Biol. 2008; 10:1470–1476. [PubMed: 19011622]
5. Lee TH, D'Asti E, Magnus N, Al-Nedawi K, Meehan B, Rak J. Microvesicles as mediators of intercellular communication in cancer-the emerging science of cellular 'debris'. Semin. Immunopathol. 2011; 33:455–467. [PubMed: 21318413]
6. Rak J. Microparticles in cancer. Semin. Thromb Hemost. 2010; 36:888–906. [PubMed: 21049390]
7. Keller S, Sanderson MP, Stoeck A, Altevogt P. Exosomes: from biogenesis and secretion to biological function. Immunol Lett. 2006; 107:102–108. [PubMed: 17067686]
8. Cocucci E, Racchetti G, Meldolesi J. Shedding microvesicles: artefacts no more. Trends Cell Biol. 2009; 19:43–51. [PubMed: 19144520]
9. Hao S, Ye Z, Li F, Meng Q, Qureshi M, Yang J, et al. Epigenetic transfer of metastatic activity by uptake of highly metastatic B16 melanoma cell-released exosomes. Exp Oncol. 2006; 28:126–131. [PubMed: 16837903]
10. Catellana D, Zobairi F, Martinez MC, Panaro MA, Mitolo V, Freyssinet JM, et al. Membrane microvesicles as actors in the establishment of a favorable prostatic tumoral niche: a role for activated fibroblasts and CX3CL1-CX3CR1 axis. Cancer Res. 2009; 69:785–793. [PubMed: 19155311]
11. Jung T, Castellana D, Klingbeil P, Cuesta Hernandez I, Vitacolonna M, Orlicky DJ, et al. CD44v6 dependence of premetastatic niche preparation by exosomes. Neoplasia. 2009; 11:1093–1105. [PubMed: 19794968]
12. Narumiya S, Tanji M, Ishizaki T. Rho signaling, ROCK and mDia1, in transformation, metastasis and invasion. Cancer Metastasis Rev. 2009; 28:65–76. [PubMed: 19160018]

13. Li B, Antonyak MA, Druso JE, Cheng L, Nikitin AY, Cerione RA. EGF potentiated oncogenesis requires a tissue transglutaminase-dependent signaling pathway leading to Src activation. Proc Natl Acad Sci USA. 2010; 107:1408–1413. [PubMed: 20080707]
14. Yuan L, Siegel M, Choi K, Khosla C, Miller CR, Jackson EN, et al. Transglutaminase 2 inhibitor, KCC009, disrupts fibronectin assembly in the extracellular matrix and sensitizes orthotopic glioblastomas to chemotherapy. Oncogene. 2007; 26:2563–2573. [PubMed: 17099729]
15. Teis D, Saksena S, Emr SD. SnapShot: the ESCRT machinery. Cell. 2009; 137:182–182. e181. [PubMed: 19345195]
16. Heasman SJ, Ridley AJ. Mammalian Rho GTPases: new insights into their functions from in vivo studies. Nat Rev Mol Cell Biol. 2008; 9:690–701. [PubMed: 18719708]
17. Roberts PJ, Der CJ. Targeting the Raf-MEK-ERK mitogen-activated protein kinase cascade for the treatment of cancer. Oncogene. 2007; 26:3291–3310. [PubMed: 17496923]
18. Muralidharan-Chari V, Clancy J, Plou C, Romao M, Chavrier P, Raposo G, et al. ARF6-regulated shedding of tumor cell-derived plasma membrane microvesicles. Curr Biol. 2009; 19:1875–1885. [PubMed: 19896381]
19. Narumiya S, Ishizaki T, Uehata M. Use and properties of ROCK-specific inhibitor Y-27632. Methods Enzymol. 2000; 325:273–284. [PubMed: 11036610]
20. Loirand G, Guerin P, Pacaud P. Rho kinases in cardiovascular physiology and pathophysiology. Circ Res. 2006; 98:322–334. [PubMed: 16484628]
21. Kawano Y, Fukata Y, Oshiro N, Amano M, Nakamura T, Ito M, et al. Phosphorylation of myosin-binding subunit (MBS) of myosin phosphatase by Rho-kinase in vivo. J Cell Biol. 1999; 147:1023–1038. [PubMed: 10579722]
22. Maekawa M, Ishizaki T, Boku S, Watanabe N, Fujita A, Iwamatsu A, et al. Signaling from Rho to the actin cytoskeleton through protein kinases ROCK and LIM-kinase. Science. 1999; 285:895–898. [PubMed: 10436159]
23. Yang N, Higuchi O, Ohashi K, Nagata K, Wada A, Kangawa K, et al. Cofilin phosphorylation by LIM-kinase 1 and its role in Rac-mediated actin reorganization. Nature. 1998; 393:809–812. [PubMed: 9655398]
24. Petrache I, Birukov K, Zaiman AL, Crow MT, Deng H, Wadgaonkar R, et al. Caspase-dependent cleavage of myosin light chain kinase (MLCK) is involved in TNF-alpha-mediated bovine pulmonary endothelial cell apoptosis. FASEB J. 2003; 17:407–416. [PubMed: 12631580]
25. Mbeunkui F, Johann DJ Jr. Cancer and the tumor microenvironment: a review of an essential relationship. Cancer Chemother Pharmacol. 2009; 63:571–582. [PubMed: 19083000]
26. Davila M, Frost AR, Grizzle WE, Chakrabarti R. LIM kinase 1 is essential for the invasive growth of prostate epithelial cells: implications in prostate cancer. J Biol Chem. 2003; 278:36868–36875. [PubMed: 12821664]
27. Davila M, Jhala D, Ghosh D, Grizzle WE, Chakrabarti R. Expression of LIM kinase 1 is associated with reversible G1/S phase arrest, chromosomal instability and prostate cancer. Mol Cancer. 2007; 6:40. [PubMed: 17559677]
28. Yoshioka K, Foletta V, Bernard O, Itoh K. A role for LIM kinase in cancer invasion. Proc Natl Acad Sci USA. 2003; 100:7247–7252. [PubMed: 12777619]
29. Bagheri-Yarmand R, Mazumdar A, Satin AA, Kumar R. LIM kinase 1 increases tumor metastasis of human breast cancer cells via regulation of the urokinase-type plasminogen activator system. Int J Cancer. 2006; 118:2703–2710. [PubMed: 16381000]
30. Clark EA, Golub TR, Lander ES, Hynes RO. Genomic analysis of metastasis reveals an essential role for RhoC. Nature. 2000; 406:532–535. [PubMed: 10952316]
31. Vega FM, Ridley AJ. Rho GTPases in cancer cell biology. FEBS Lett. 2008; 582:2093–2101. [PubMed: 18460342]
32. Micuda S, Rösel D, Ryska A, Brábek J. ROCK inhibitors as emerging therapeutic candidates for sarcomas. Curr Cancer Drug Targets. 2010; 10:127–134. [PubMed: 20088801]
33. Fackler OT, Grosse R. Cell motility through plasma membrane blebbing. J Cell Biol. 2008; 181:879–884. [PubMed: 18541702]

34. Di Vizio D, Kim J, Hager MH, Morello M, Yang W, Lafargue CJ, et al. Oncosome formation in prostate cancer: association with a region of frequent chromosomal deletion in metastatic disease. Cancer Res. 2009; 69:5601–5609. [PubMed: 19549916]

35. Charras GT, Hu CK, Coughlin M, Mitchison TJ. Reassembly of contractile actin cortex in cell blebs. J Cell Biol. 2006; 175:477–490. [PubMed: 17088428]

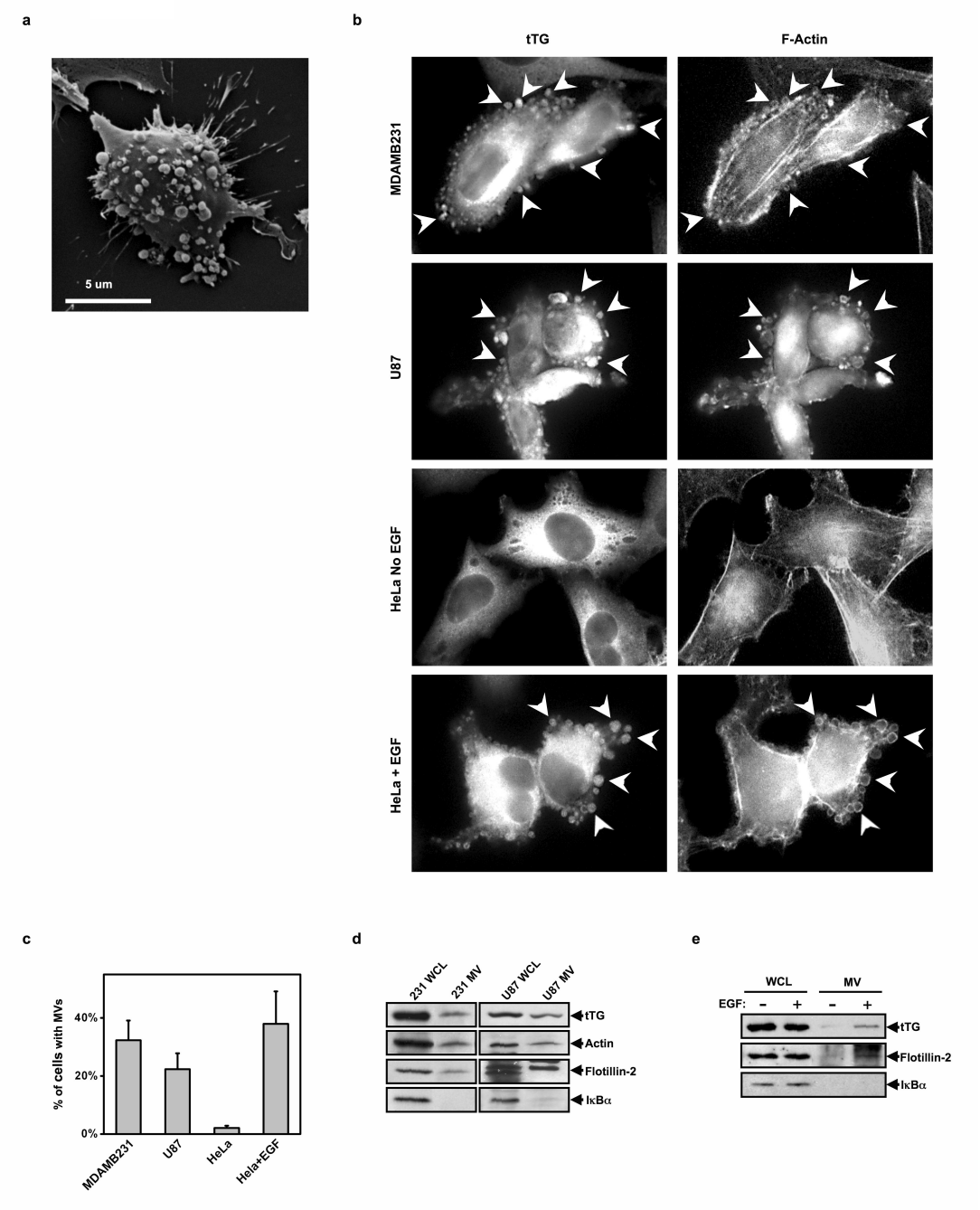

Figure 1.

Different human cancer cell lines generate MVs. (**a**) A scanning electron microscopy image of a MDAMB231 cell shedding MVs from its surface. (**b**) Immunofluorescent images of serum-starved and EGF-stimulated MDAMB231, U87, and HeLa cells stained with a tTG antibody and rhodamine-conjugated phalloidin (to detect F-actin). Some of the most pronounced MVs are denoted with arrows. (**c**) Quantification of MV production by the cells in **b**. (**d**) Cultures of serum-starved MDAMB231 or U87 cells, and (**e**) cultures of serum-starved or EGF-stimulated HeLa cells, were lysed and the MVs shed into the medium by

these cells were isolated and then lysed. The whole cell lysates (WCLs) and the MV lysates were immunoblotted with tTG, actin, flotillin-2, and IκBα antibodies.

a

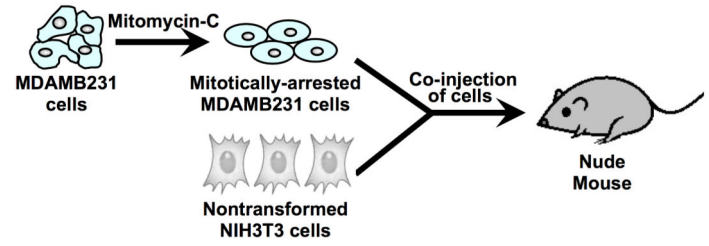

b

Cells Injected	Tumors formed/ Injection	Cells Injected	Tumors formed/ Injection
Naïve 231 cells	4/4	Mito-C-treated 231 cells	0/6
Naïve NIH3T3 cells	0/6	Mito-C-treated 231 cells + NIH3T3 cells	3/6

c

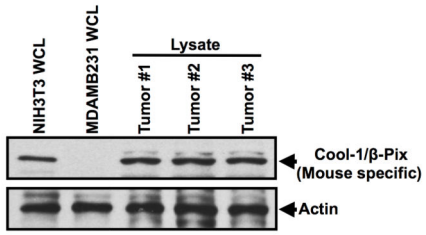

Figure 2.

MVs promote tumor formation. (**a**) Schematic of the tumor-formation assays performed to determine the role of MVs in mediating tumor growth. Mitotically-arrested MDAMB231 cells (using mitomycin C) were co-injected into nude mice with an equal number of normal (non-transformed) NIH3T3 fibroblasts. The ability of the MVs generated by the mitotically-arrested MDAMB231 cells to confer upon the recipient NIH3T3 fibroblasts the ability to form tumors was read-out. (**b**) Table showing the results of a tumor-formation assay performed as outlined in **a**. Half of the mice injected with mitotically-arrested MDAMB231 and NIH3T3 cells (*Mito-C-treated 231 cells + NIH3T3 cells*) formed tumors, whereas mice injected with the mitotically-arrested cancer cells (*Mito-C-treated 231 cells*) or the NIH3T3 cells (Naïve *NIH3T3 cells*), alone, failed to form tumors. Naïve MDAMB231 cells (*Naïve 231 cells*) were injected into the animals to confirm the tumor-promoting ability of these cells. (**c**) Lysates generated from cultures of NIH3T3 mouse fibroblasts and of MDAMB231 human breast cancer cells, as well as from the three tumors that formed as a result of combining the mitotically-arrested MDAMB231 and NIH3T3 cells (*Mito-C-treated 231 cells + NIH3T3 cells*) were immunoblotted with an antibody that recognizes only the mouse form of Cool-1/β-Pix (*top panel*). Note that the Cool-1/β-Pix protein can be detected in each

of the tumor samples, suggesting that the tumor masses are made-up of NIH3T3 mouse fibroblasts. The blot was then re-probed with actin to confirm equal loading (*bottom panel*).

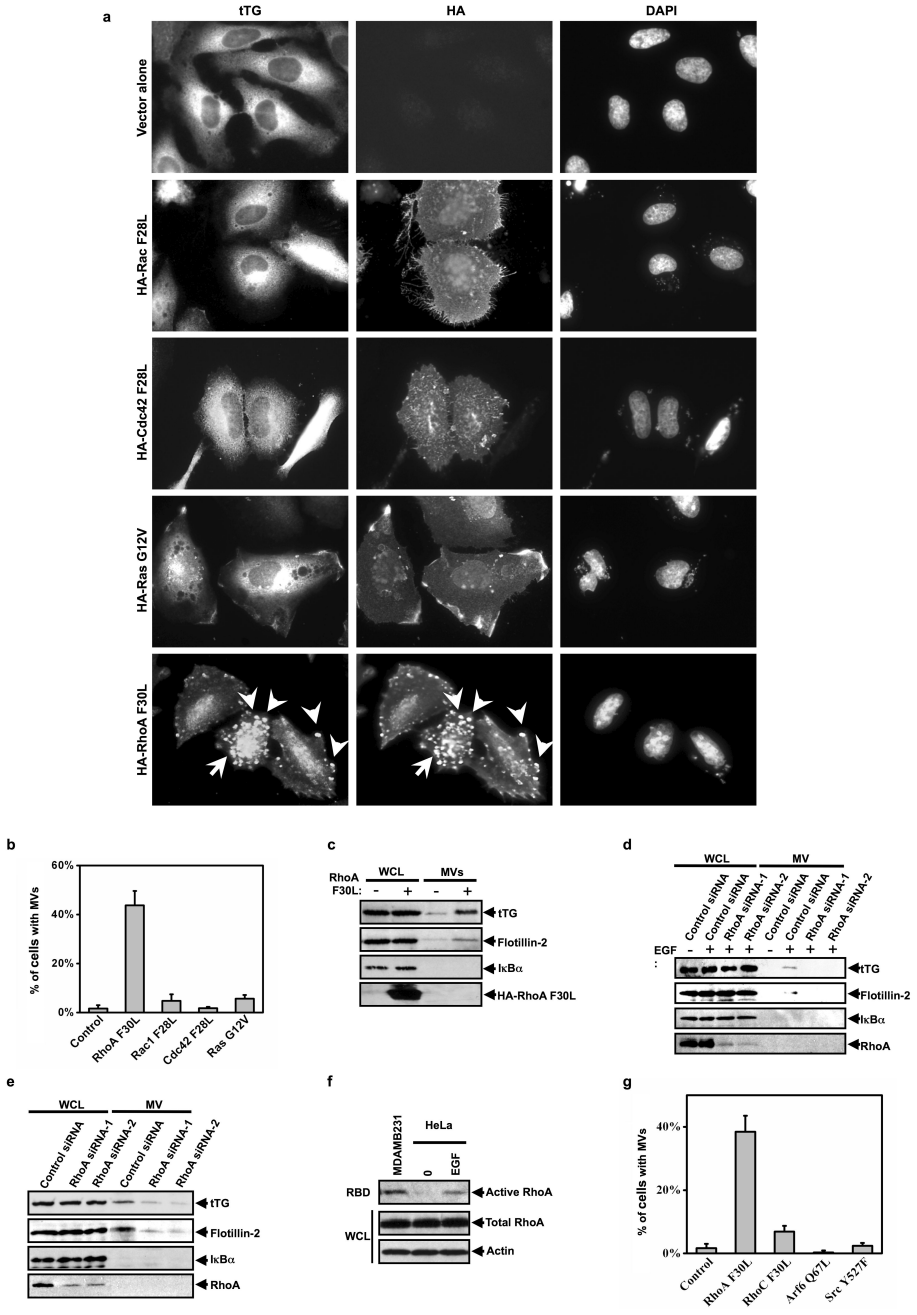

Figure 3.

MVs generation in human cancer cells is RhoA-dependent. (**a**) HeLa cells ectopically expressing HA-tagged forms of activated Rac (Rac F28L), Cdc42 (Cdc42 F28L), Ras (Ras G12V), or RhoA (RhoA F30L) were immunostained with tTG and HA antibodies and DAPI was used to label nuclei. Some of the MVs are indicated with arrows. (**b**) Quantification of MV production by the transfectants shown in **a**. (**c**) The whole cell lysates (WCLs) and the MVs collected from serum-starved HeLa cells ectopically expressing the vector alone or HA-tagged RhoA F30L were immunoblotted as indicated. (**d, e**) The whole cell lysates

(WCLs) and the MV lysates collected from serum-starved cultures of control siRNA or RhoA siRNA expressing (**d**) HeLa cells or (**e**) MDAMB231 cells, that had been treated without or with EGF, as indicated, were immunoblotted with the indicated antibodies. (**f**) RBD binding assays were performed on the extracts from serum-starved or EGF-stimulated MDAMB231 cells and HeLa cells, as indicated. The amount of activated or total RhoA was detected by immunoblotting the RBD samples and the whole cell lysates (WCL) with a RhoA antibody. To confirm equal input, the membrane was re-probed with an actin antibody. (**g**) Quantification of MV production by HeLa cells ectopically expressing the dominant-active forms of the indicated signaling proteins. The histograms show mean ± SD.

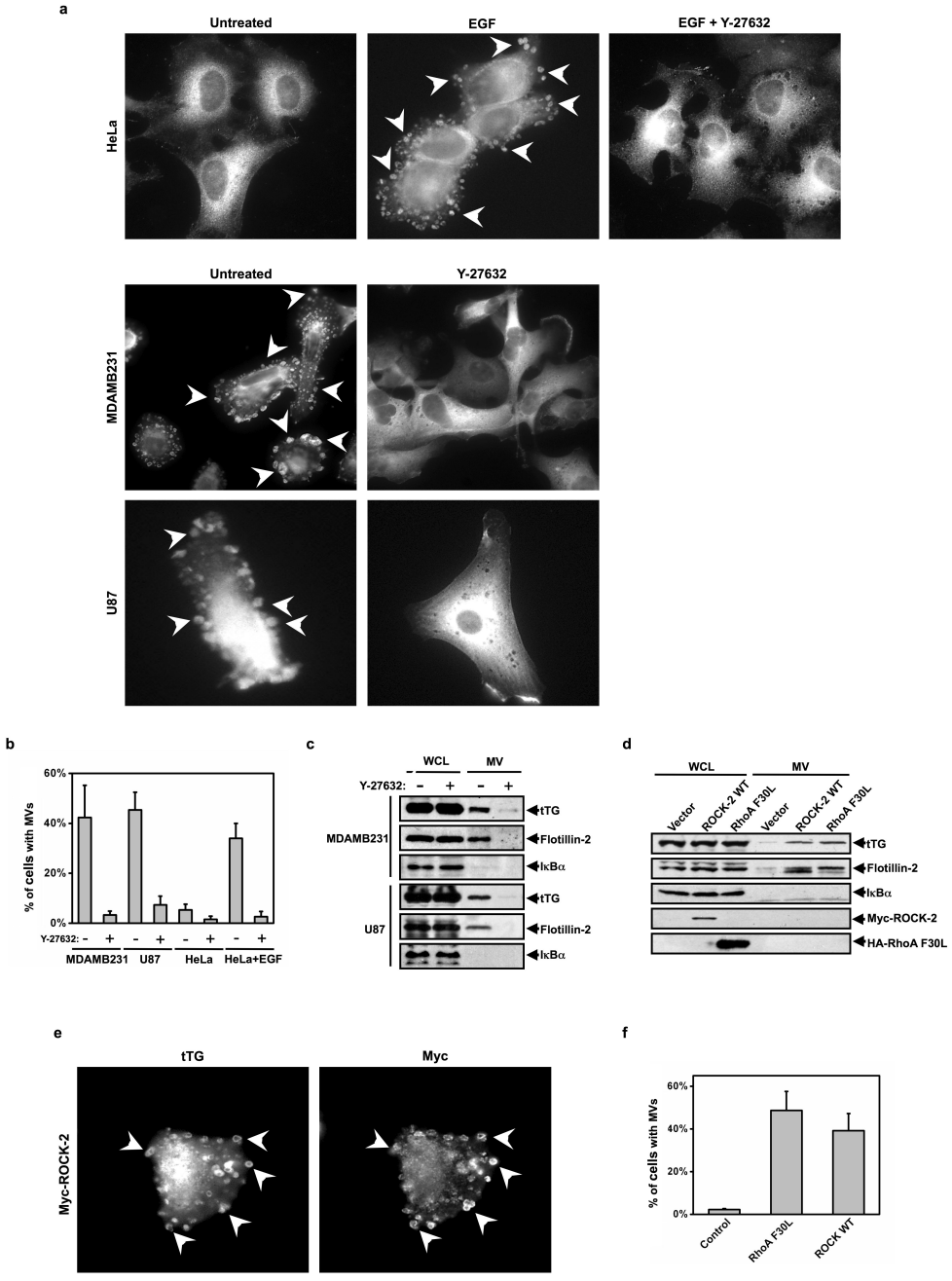

Figure 4.

ROCK is downstream from RhoA in the pathway leading to MV formation. **(a)** Serum-starved cultures of HeLa, MDAMB231, and U87 cells were treated with or without Y-27632. The HeLa cells were further treated without or with EGF, as indicated, and then the cells were stained for tTG to identify MVs, some of which are denoted with arrows. **(b)** Quantification of MV production by the cells shown in **a**. (**c**) The whole cell lysates (WCLs) and MV lysates generated from serum-starved MDAMB231 and U87 cells that had been treated without or with Y-27632 were immunoblotted as indicated. (**d, e**) Duplicate sets of

HeLa cells overexpressing the vector alone, Myc-tagged wild-type ROCK-2 (ROCK WT), or HA-tagged RhoA F30L were generated. (**d**) One set was lysed (WCLs) and the MVs shed into the medium by the transfectants were isolated and then lysed. The WCLs and the MV lysates were immunoblotted as indicated. (**e**) Another set was immunostained with tTG and Myc antibodies. Arrows denote pronounced MVs. (**f**) Quantification of MV production by the cells shown in **e**. The histograms show mean ± SD.

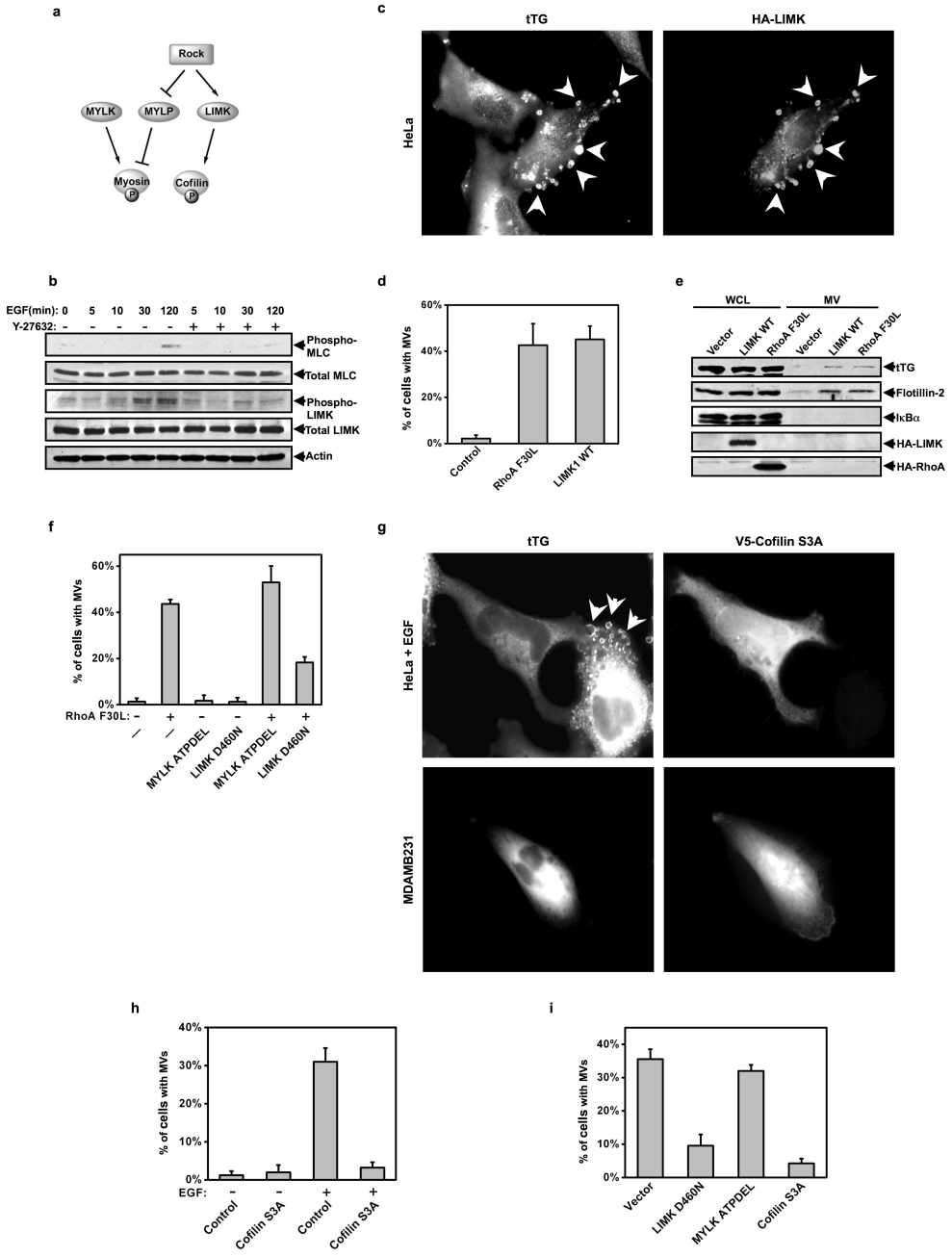

Figure 5.

LIMK and cofilin are the critical downstream effectors of ROCK that regulate MV formation. (**a**) Illustration of the ROCK-signaling pathway. (**b**) The extracts collected from serum-starved HeLa cells that had been stimulated with EGF for the indicated lengths of time, without or with Y-27632, were immunoblotted as indicated. (**c-e**) Multiple sets of HeLa cells ectopically expressing the vector alone, HA-tagged wild-type LIMK (LIMK WT), or RhoA F30L were generated. (**c**) One set was immunostained with tTG and HA antibodies and DAPI was used to label nuclei. Shown is an image of a transfectant. (**d**)

Quantification of MV production by the cells in **c**. (**e**) The whole cell lysates (WCLs) and the MV lysates collected from another set of the transfectants were immunoblotted as indicated. (**f**) HeLa cells transiently expressing the vector alone (-) or RhoA F30L were then further transfected with either the vector-only, a dominant-negative form of LIMK (LIMK D460N), or a dominant-negative form of MYLK (MYLK ATPDEL), as indicated, and then were immunostained for tTG to identify MVs. MV production by the transfectants was determined and then graphed. (**g-i**) Multiple plates of serum-starved or EGF-stimulated HeLa cells or MDAMB231 cells expressing various constructs including the vector-only, V5-tagged cofilin S3A, LIMK D460N, and MYLK APTDEL were generated and then fixed. The cells were then stained with tTG to identify MVs and either V5, Myc, or HA antibodies to identify transfectants. (**g**) Images of EGF-stimulated HeLa cells and serum-starved MDAMB231 cells ectopically expressing V5-tagged cofilin S3A. Note that the cells expressing V5-tagged cofilin S3A lack MVs. (**h**) Quantification of MV production by serum-starved or EGF-stimulated HeLa cells ectopically expressing the vector alone (control) or V5-tagged cofilin S3A. (**i**) Quantification of MV production by serum-starved MDAMB231 cells ectopically expressing the indicated constructs. The histograms show mean ± SD.

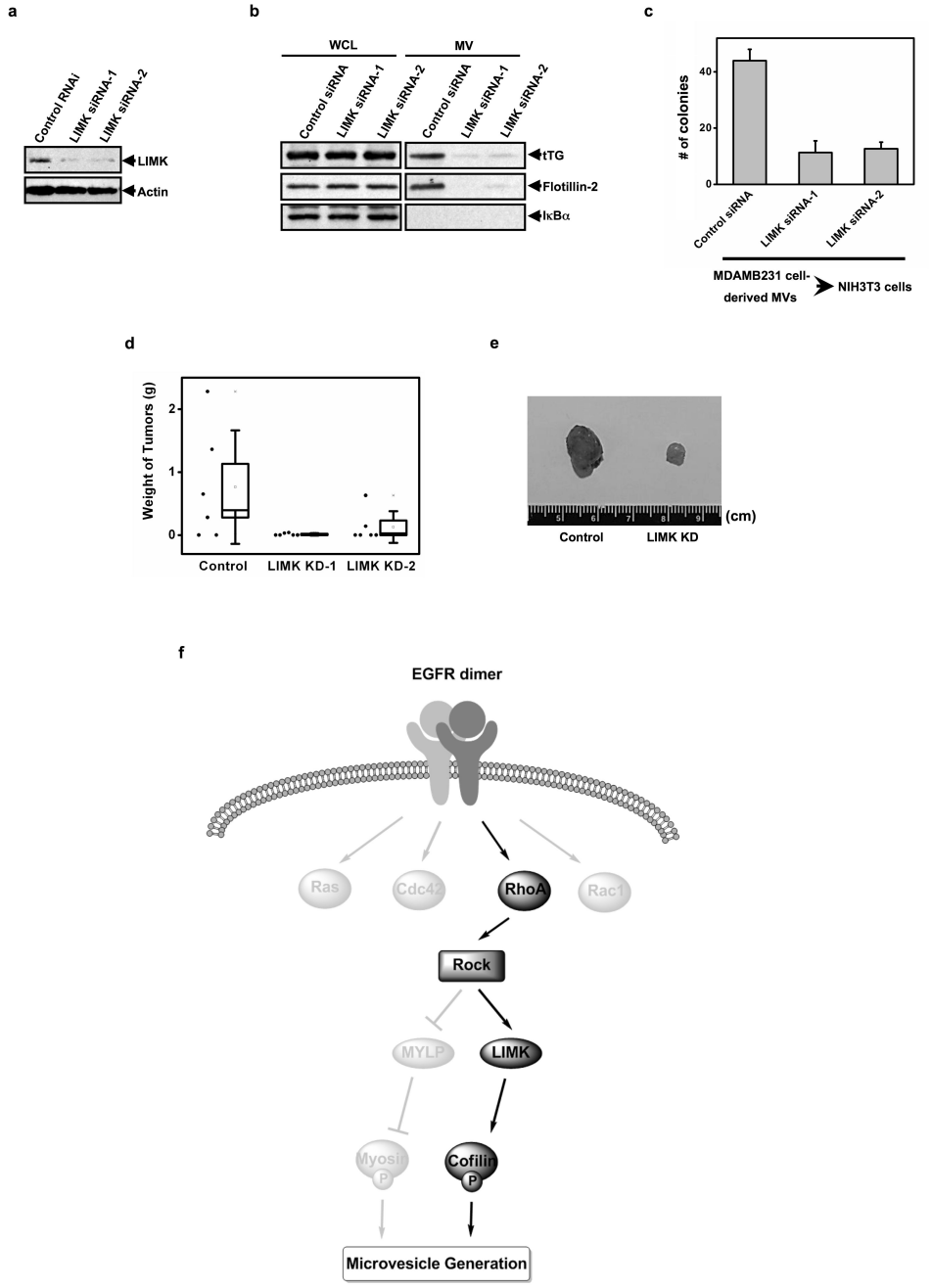

Figure 6.

Knocking-down LIMK in MDAMB231 cells suppresses the MV-induced transformation of recipient fibroblasts *in vitro* and *in vivo*. (**a**) MDAMB231 cells stably expressing control siRNA or LIMK siRNAs were lysed and immunoblotted with LIMK and actin antibodies. (**b-d**) Multiple cultures of each of the MDAMB231 cells stably expressing control siRNA or the LIMK siRNAs were prepared. (**b**) The whole cell lysates (WCLs) and the MVs collected from one set of the clones that had been serum-starved for 1 day were immunoblotted as indicated. (**c**) Intact MVs were isolated from the medium of a second set of the clones that

had been serum-starved. NIH3T3 fibroblasts incubated with each of the MV preparations were then subjected to anchorage-independent growth assays. The colonies that formed for each condition were counted. (**d**) A third set of the stable cell lines were mitotically-arrested (using mitomycin C), combined with an equal number of NIH3T3 cells, and then were injected into nude mice. The resulting tumors that formed for each condition were weighed, averaged, and then graphed. The black dots located to the left of each plot indicate the weight of individual tumors. The histograms show mean ± SD. (**e**) Image of tumors that formed in **d**. (**f**) Diagram of the signaling pathway that triggers MV generation/shedding in cancer cells.